Environmental Science & Technology

Article

pubs.acs.org/est

Osmotic Ballasts Enhance Faradaic Efficiency in Closed-Loop, Membrane-Based Energy Systems

Ryan S. Kingsbury and Orlando Coronell*

Department of Environmental Sciences and Engineering, Gillings School of Global Public Health, The University of North Carolina at Chapel Hill, Chapel Hill, North Carolina 27599, United States

Supporting Information

ABSTRACT: Aqueous processes for energy storage and conversion based on reverse electrodialysis (RED) require a significant concentration difference across ion exchange membranes, creating both an electrochemical potential and an osmotic pressure difference. In closed-loop RED, which we recently demonstrated as a new means of energy storage, the transport of water by osmosis has a very significant negative impact on the faradaic efficiency of the system. In this work, we use neutral, nonpermeating solutes as "osmotic ballasts" in a closed-loop concentration battery based on RED. We present experimental results comparing two proof-of-concept ballast molecules, and show that the ballasts reduce, eliminate, or reverse the net transport of water through the membranes when cycling the battery. By mitigating osmosis, faradaic and round-trip energy efficiency are more than doubled, from 18% to 50%, and 7% to 15%, respectively in this nonoptimized system. However, the presence of the ballasts has a slightly negative impact on the open circuit voltage. Our results suggest that balancing osmotic pressure using noncharged solutes is a promising approach for significantly reducing faradaic energy losses in closed-loop RED systems.

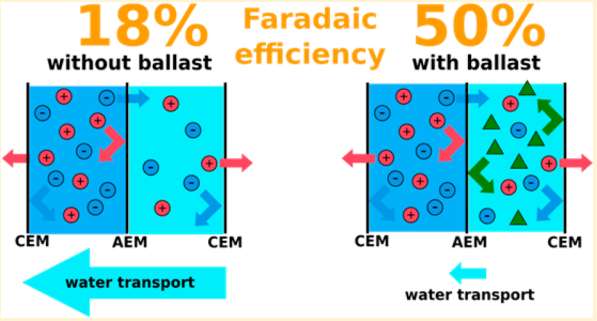

INTRODUCTION

There is a widely acknowledged need for scalable and economical means of storing electric energy to support the increasing deployment of intermittent energy sources.[1] Reversible desalination is a novel approach to this challenge that can be used to store energy using electrolyte concentration gradients. In previous work,[2] we demonstrated a concentration battery that uses electrodialysis (ED) to convert electric energy into a concentration difference between two salt solutions separated by ion exchange membranes, and reverse electrodialysis (RED) to convert this chemical potential energy back into electricity (Figure 1). A similar concept has recently been proposed by van Egmond et al.[3]

In addition to the salt concentration difference, an osmotic pressure difference is created between the two salt solutions, resulting in unwanted water transport across the ion exchange membranes toward the concentrated salt solution. Water transport by osmosis has been acknowledged as a source of energy loss in the context of RED for energy generation,[3−6] but its impact on energy efficiency is often neglected. This is because RED-based energy generation is a flow-through, steady-state process, in which the limited osmosis that occurs as the solutions flow through the membrane stack is counteracted to some extent by electro-osmosis.[4,6] In contrast, RED-based energy storage is a closed-loop, nonsteady state process, in which the unwanted water transport between solutions accumulates over time and results in a significant loss of efficiency (Figure 1).[2]

In principle, water transport could be controlled by applying differential pressure between the two solutions. However, this approach would create an additional loss of efficiency by increasing the required pumping energy, and would be difficult to implement in full-scale RED systems due to the need for thin membranes with low resistance to ion transport. Alternatively, it may be possible to modify ion exchange membranes to inhibit water transport, but since ion conduction takes place through hydrophilic domains in the polymer, it seems unlikely that this approach could completely prevent osmosis as long as a driving force exists.

To address the problem of unwanted osmosis in salinity-gradient energy systems, we propose to add an "osmotic ballast" (a noncharged solute) to the dilute electrolyte solution to balance the osmotic pressure between dilute and concentrated solutions (Figure 1). This approach eliminates the driving force for water transport, avoiding the need to develop new materials or stack designs. We present experimental results obtained using two different ballasts that demonstrate that osmotic ballasts lead to significant improvements in the energy efficiency of a RED-based concentration battery. We also illustrate directions for further improving the osmotic ballast approach for the control of unwanted osmosis.

Received: July 25, 2016
Revised: December 20, 2016
Accepted: December 23, 2016
Published: December 23, 2016

DOI: 10.1021/acs.est.6b03720
Environ. Sci. Technol. 2017, 51, 1910−1917

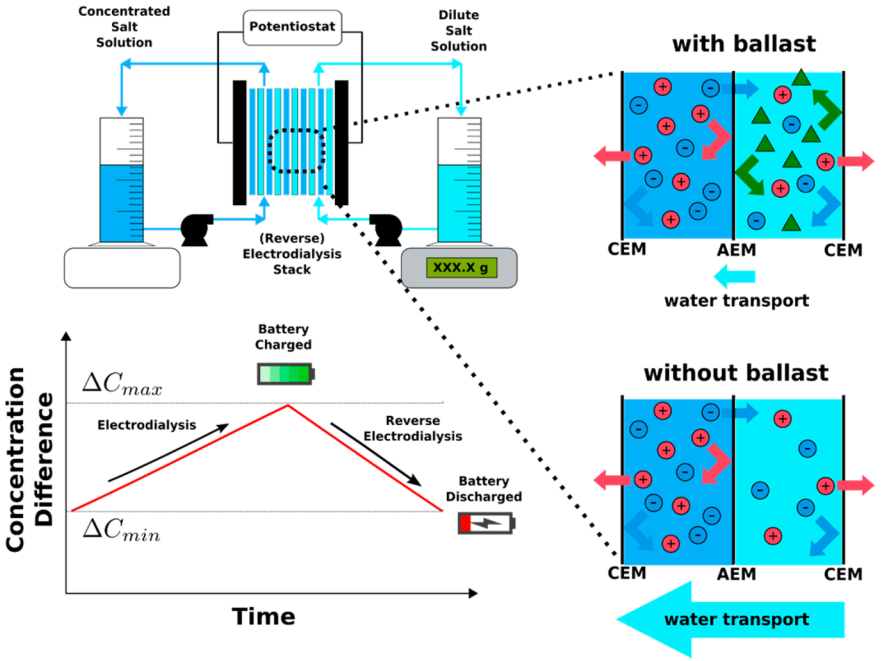

Figure 1. Schematic of experimental apparatus (upper left), graphical representation of electrodialytic charge−discharge cycle under constant current (lower left), and conceptual illustration of osmotically balanced salt solutions (right). Ballast molecules (green triangles) take the place of water molecules in the dilute solution, thus equalizing the osmotic pressures on both sides of the membrane.

MATERIALS AND METHODS

Osmotic Ballasts. An ideal osmotic ballast is a substance that is highly soluble in aqueous solution, has a low viscosity (so as not to adversely impact the electrical conductivity of the dilute solution and pumping energy required to circulate it), does not permeate through the ion exchange membranes, and has relatively low cost and toxicity. Ethylene glycols are highly miscible with water, compatible with polymeric ion exchange membranes,[7,8] and are widely used in applications such as antifreezes and deicing solutions where manipulation of the osmotic pressure is desired.[9] Accordingly, in this work we selected two ethylene glycol oligomers (n = 1 and n = 4, hereinafter mono-EG and tetra-EG, respectively) as illustrative ballasts. The ethylene glycol oligomers (99.5%+ purity) were purchased from Acros Organics (Geel, Belgium) and used without further purification. Relevant properties of these osmotic ballasts are provided in Table 1.

Preparation of Osmotically Balanced Solutions. All ballasted dilute solutions were prepared with reference to a concentrated salt solution containing 0.513 M sodium chloride in ultrapure water (≥18 MΩ.cm), with no ballast added.

Dilute salt solutions were prepared using ultrapure water, sodium chloride (99%+ purity), and either mono-EG or tetra-EG in such a way that the molar concentration of salt remained constant at 0.257 M, regardless of the amount of ballast added.

Given that in our tests ballast was added to the dilute salt solution to minimize osmosis from the dilute to the concentrated salt compartments, we prepared dilute salt solutions with a ballast concentration ($C_{B,OB}$) equal to that theoretically needed to achieve osmotic balance with the concentrated salt solution. For long-term operation of the battery, it would potentially be desirable to select $C_{B,OB}$ according to the average osmotic pressure over the full charge−discharge cycle. However, since this value of osmotic pressure is impossible to determine a priori, we calculated $C_{B,OB}$ based on the initial (discharged battery) state. The $C_{B,OB}$ calculations were performed on the basis of the Gibbs equation[12] which describes the osmotic pressure (π, Pa) of an aqueous solution as given by

$$\pi = -\frac{RT}{V_w}\ln \gamma_w x_w \quad (1)$$

where V_w ($m^3.mol^{-1}$), x_w (dimensionless) and γ_w (dimensionless) are the molar volume, mole fraction and activity coefficient of water, respectively, R is the universal gas constant (8.314 L.atm.K^{-1}.mol^{-1}), and T (K) is the temperature (see illustrative calculations in the Supporting Information). For each of the two ballasts, in addition to preparing dilute salt solutions containing 100% of $C_{B,OB}$ (i.e., 2.7%v/v and 7.6%v/v for mono-EG and tetra-EG, respectively), we also prepared dilute salt solutions containing 150% and 200% of $C_{B,OB}$. Solutions with a ballast concentration greater than $C_{B,OB}$ were prepared in order to compensate for the tendency of the ballast to diffuse through the ion exchange membranes toward the concentrated salt solution compartment.

Concentration Battery Testing Procedure. A concentration gradient battery based on RED was constructed using a commercially available electrodialysis stack (PCCell 64002, PCCell GmbH, Germany) containing 10 pairs of cation and

Table 1. Properties of Ethylene Glycol Oligomers Used As Osmotic Ballasts in This Study

oligomer	molecular weight (g mol^{-1})	self-diffusion coefficient (10^{-5} $cm^2.s^{-1}$)	viscosity at room temperature (cP)[a]
mono-EG (n = 1)	62.07[10]	0.95[10]	1.5[10]
tetra-EG (n = 4)	194.23[11]	0.18[11]	2.0[11]

[a]Viscosity of a 10% by weight mixture of ethylene glycol oligomer in water.

DOI: 10.1021/acs.est.6b03720
Environ. Sci. Technol. 2017, 51, 1910−1917

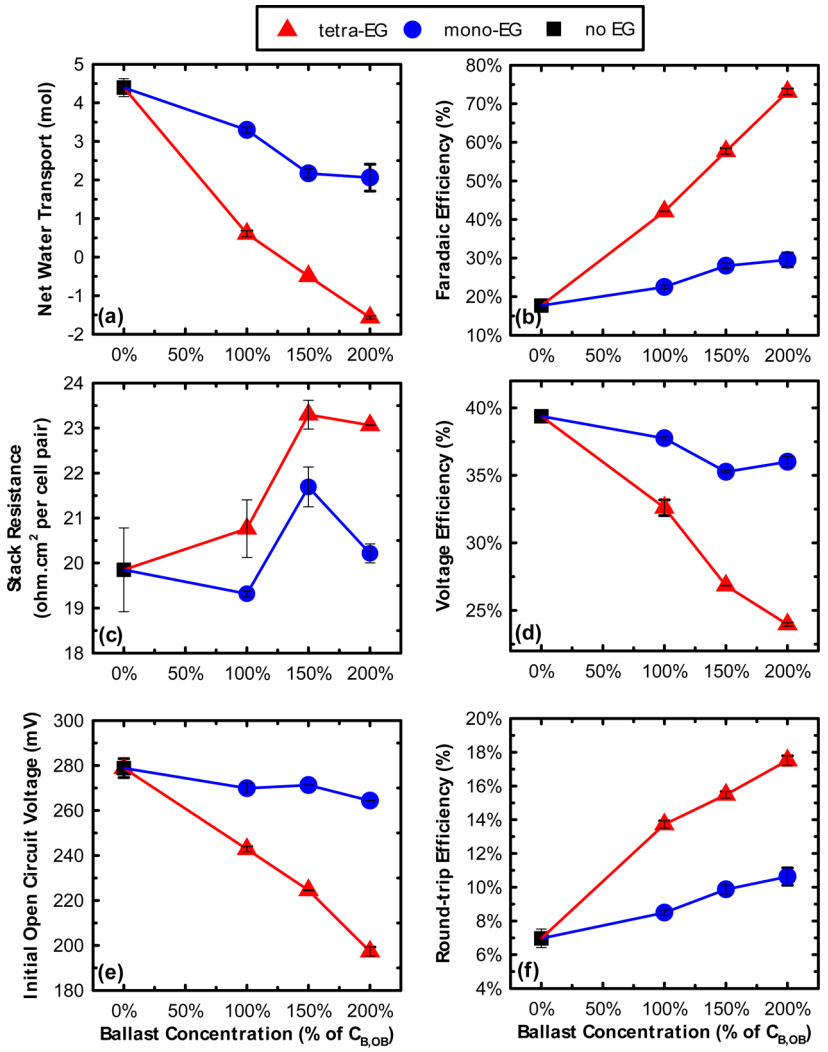

Figure 2. Battery performance over complete charge−discharge cycles as a function of mono-EG and tetra-EG ballast concentration. The ballast concentrations are normalized to the theoretical concentration ($C_{B,OB}$) needed to achieve osmotic balance between the concentrated and dilute salt solutions. (a) Net water transport. (b) Faradaic efficiency. (c) Stack resistance. (d) Voltage efficiency. (e) Initial open circuit voltage. (f) Round-trip energy efficiency. Data points and error bars (some of which are covered by the symbols) represent the average and standard deviation, respectively, of two replicates.

anion exchange membranes (AEMs and CEMs, respectively) plus one additional CEM and mixed-metal oxide coated titanium electrodes. Concentrated and dilute salt solutions were circulated through the stack in a closed-loop (Figure 1) from respective feed reservoirs, each with an initial solution volume of approximately 180 mL. Ag/AgCl reference electrodes (BaSi, Inc. RE-5B) were placed near the exterior face of the outermost membranes and were used to measure the potential across the membrane stack. The starting salt concentrations for all cycles were 0.513 and 0.257 M for the concentrated and dilute solutions, respectively, approximating the conditions used in previous work.[2]

The concentration battery was taken through a single, potential-limited, galvanostatic charge−discharge cycle by means of a potentiostat (VMP3, Bio-Logic Science Instruments, France). We began each cycle by performing ED to charge the battery, increasing the concentration difference until the open circuit voltage (OCV) of the stack reached the target potential (425 mV). The target ending potential of 425 mV was chosen based on the potential that could be achieved within approximately 2 h of charging time. Then, we reversed the current, and the battery was discharged by RED until it returned to the potential at the beginning of the test as determined by the OCV of the stack containing the starting salt solutions. The corresponding discharge times varied between 35 and 100 min. The solution volumes in the concentrated and dilute feed reservoirs (graduated cylinders) were recorded periodically throughout each charge−discharge cycle, while the conductivity of both solutions was measured at the beginning and end of the cycle using a benchtop meter (Accumet XL60 with conductivity probe, Hudson, MA). The overall resistance of the battery was measured at the beginning and end of each charge−discharge cycle using linear sweep voltammetry. All charge−discharge cycles were conducted at 20 °C.

As described in our previous work,[2] there is an optimum current density that maximizes the round-trip energy efficiency of this type of charge−discharge cycle. Preliminary experiments without ballast were used to determine the optimal current density for this stack (7.0 $A.m^{-2}$, see Supporting Information), and all subsequent tests were conducted at this current density. Duplicate cycles were performed for each ballast type and concentration.

DOI: 10.1021/acs.est.6b03720
Environ. Sci. Technol. 2017, 51, 1910−1917

Determination of Water and Ballast Transport Across Ion Exchange Membranes. The net transport of water during each charge−discharge cycle was determined by monitoring the volumes of the concentrated and dilute solutions in their respective feed reservoirs. The mass of the dilute solution was also monitored by placing its graduated cylinder on an electronic balance (Ohaus N1H110). We calculated the net transport of water from the measured volume changes in the dilute salt solution reservoir, cross-checked against the measured changes in mass of the dilute solution and volume in the concentrated solution (see example calculation in the Supporting Information). We assumed that the net water transport observed was primarily the result of osmosis. While some transport of water also occurs as electro-osmosis (the dragging along of water by salt molecules), electro-osmosis follows the direction of the ionic current and is thus reversible. As faradaic (current) efficiency increases, the number of coulombs of current passed in each direction becomes nearly equal. Therefore, the net solution volume change over the course of a charge−discharge cycle approaches that due to true osmosis as faradaic efficiency approaches 100%.

The net transport of ballast during each charge−discharge cycle was determined by measuring the total organic carbon (TOC) content in the concentrated and dilute reservoirs at the beginning and end of the cycle. TOC content was measured using a TOC-V analyzer (Shimadzu, Atlanta, GA). We used the TOC concentrations in combination with the starting and ending volumes of each solution to determine the net ballast mass transported from one solution to the other. Example calculations of ballast transport are provided in the Supporting Information.

RESULTS AND DISCUSSION

Osmosis and Faradaic Efficiency. The impact of the addition of osmotic ballast to the dilute salt solution on the performance achieved during the charge−discharge cycles is summarized in Figure 2. First, we focus our attention on the effect of ballast addition on osmosis and faradaic (current) efficiency. As shown in Figure 2a, the addition of either mono-EG or tetra-EG ballast at 100% of $C_{B,OB}$ reduced the net transport of water from the dilute to the concentrated salt compartment by 25% and 86%, respectively, compared to the water transport that occurred when no ballast was used.

Increasing the ballast concentrations above $C_{B,OB}$ continued to decrease the net water transport, with tetra-EG causing inverted osmosis (i.e., transport of water from the concentrated to the dilute salt solution as indicated by negative values in Figure 2a). The greater effectiveness of tetra-EG compared to mono-EG at reducing water transport can be attributed to the larger size, and corresponding lower diffusivity, of tetra-EG (Table 1). The larger size and lower diffusivity of tetra-EG, compared to mono-EG, likely allowed tetra-EG to be rejected more effectively by the ion exchange membranes, and therefore to maintain a more stable ballast concentration in the dilute salt solution.

Figure 2b shows that the faradaic efficiency was always higher when ballast was added to the dilute solution. Faradaic efficiency (η_I, dimensionless) is defined as the ratio between the quantity of charge extracted from the concentration battery during the discharge stage (RED) and the quantity of charge needed to complete the charging stage (ED). As such, η_I can be calculated by integrating current with respect to time according to[13]

$$\eta_I = \frac{\int_0^{t_d} I_d dt}{\int_0^{t_c} I_c dt} \quad (2)$$

where t (s) is the duration of the charging or discharging stages, I (A) is the current at any point in time during the charging or discharging stages, and the subscripts c and d indicate the charging and discharging stages, respectively.

Given that osmosis from the dilute to the concentrated solution reduces the salinity gradient between the two solutions (i.e., discharges the battery), but does not produce electric current, osmosis effectively reduces faradaic efficiency.[2] Accordingly, given that ballast addition reduced osmosis from the dilute to the concentrated solution, ballast addition also increased faradaic efficiency. Specifically, mono-EG increased faradaic efficiency from 18% with no ballast to a maximum of 30%, while tetra-EG roughly quadrupled the faradaic efficiency to a maximum of 73%. However, in the case of tetra-EG, the highest efficiencies corresponded with the occurrence of inverted osmosis which had the effect of spontaneously increasing the salinity gradient, since water transport occurred from the concentrated to the dilute salt solution. As such, ballast addition shortened the charging time (electrodialysis stage) and prolonged the discharging time (reverse electrodialysis stage), leading to a higher faradaic efficiency.

While inverted osmosis could be useful in some applications (e.g., production of salt-free water by forward osmosis), sustainable, multicycle operation of the concentration battery is only possible when osmosis is reduced to nearly zero. For tetra-EG, the results in Figure 2a indicate that zero osmosis should occur at a ballast concentration equal to approximately 125% of $C_{B,OB}$. At this tetra-EG concentration, the faradaic efficiency was approximately 50%, implying that the corresponding 50% faradaic efficiency loss can be attributed to salt diffusion through the membranes. Since salt diffusion reduces the salinity gradient between the two solutions (i.e., discharges the battery), salt diffusion prolongs the charging time and shortens the discharge time. By decreasing the numerator and increasing the denominator in eq 2, salt diffusion thus reduces faradaic efficiency.[2] Given that the faradaic efficiency at zero osmosis is 50%, we conclude that osmosis and salt diffusion play a roughly equal role in faradaic energy loss for this system. Previously reported modeling results from an energy storage system similar to the one discussed here, but with different membranes,[2] showed that osmosis played a dominant role in faradaic efficiency loss compared to salt diffusion. Taken together, these two findings suggest that the relative importance of osmosis and diffusion in RED-based energy storage is highly dependent on the type of membranes used.

Stack Resistance and Voltage Efficiency. Next, we consider the impact of the ballast on the overall resistance of the concentration battery and its voltage efficiency. Figure 2c shows that when either mono-EG or tetra-EG was added to the dilute salt solution at 100% of $C_{B,OB}$, the stack resistance was within experimental error of the case where no ballast was added (3.2 Ω). At higher concentrations, resistance with tetra-EG showed a modest increase, with a maximum stack resistance of 3.8 Ω at 150% of $C_{B,OB}$ and a similar resistance at the highest ballast concentration. The trend for mono-EG was similar to that for tetra-EG, but after having a maximum resistance of 3.6 Ω at 150% of $C_{B,OB}$, a modest decrease in the stack resistance to 3.3 Ω was observed at the highest ballast concentration.

DOI: 10.1021/acs.est.6b03720
Environ. Sci. Technol. 2017, 51, 1910−1917

Toward evaluating the causes for the general increase in stack resistance observed when ballast was added to the dilute salt solution, we examined the effect that the ballast has on the conductivity of the dilute salt solution. While the average conductivity of the dilute salt solution containing no ballast (between the beginning and the end of the charge−discharge cycle) was 24.7 $mS.cm^{-1}$, the average conductivity of the dilute salt solution ballasted with tetra-EG was 21.2, 19.8, and 18.6 $mS.cm^{-1}$ when tetra-EG was added at 100%, 150%, and 200% of $C_{B,OB}$, respectively. Similarly, the corresponding average conductivities when mono-EG was added were 23.6, 23.1, and 22.7 $mS.cm^{-1}$. Therefore, ballast addition to the dilute salt solution decreased solution conductivity. This observation is consistent with the fact that the viscosity of mixtures of mono-EG or tetra-EG with pure water is known to increase monotonically with concentration,[10,11] and that in general, increased viscosity decreases the ionic conductivity of a solution (e.g., Walden's rule).[14]

To further investigate the causes of changes in stack resistance with ballast addition, we performed resistance measurements on individual membranes when in contact with solutions with and without ballast (see Supporting Information). These tests showed that ballast addition caused a modest monotonic increase in membrane resistance with increasing ballast concentration, where the area resistance at the highest ballast concentration was ∼1 $\Omega.cm^2$ higher than the area resistance in pure saltwater. For the AEM, the impacts of mono-EG and tetra-EG on resistance were similar. For the CEM, the impact of tetra-EG was somewhat greater than that of mono-EG. However, the experimental uncertainty in the measured membrane resistance was similar in magnitude to the observed change in resistance with ballast addition. Nevertheless, the observed increase in area resistance with ballast addition was generally consistent with expectations. For example, the area resistance of AEMs[15] and CEMs[16] was previously shown to increase when they were exposed to electrolyte solutions containing increasing concentrations of diethylene glycol.

Next, we predicted the overall stack resistance for all conditions tested using the measured solution conductivity and membrane resistance, and found that the predicted resistances were not significantly different from the measured stack resistance (see Supporting Information). Therefore, we conclude that, within experimental error, the increase in overall stack resistance with ballast addition was explained by the increases in resistance of both salt solution and membranes. Nevertheless, we are not certain of what caused the observed decrease in overall stack resistance when the mono-EG concentration was increased from 150% to 200% of $C_{B,OB}$.

The voltage efficiency results are presented in Figure 2d, which shows that in general, the voltage efficiency decreased when ballast was added to the dilute solution. The voltage efficiency (η_V, dimensionless) is defined as the ratio between average battery voltage during the discharge stage and the average battery voltage during the charging stage, as given by[13]

$$\eta_V = \frac{\frac{1}{t_d}\int_0^{t_d} E_d dt}{\frac{1}{t_c}\int_0^{t_c} E_c dt} \quad (3)$$

where E (V) is the battery voltage at any point in time during the charging or discharging stages. E is related to the OCV of the battery by

$$E = \mathrm{OCV} \pm iR \quad (4)$$

where i (A) is the electric current and R (Ω) is the stack resistance. By creating an additional potential drop, the stack resistance causes the battery voltage E to increase (during the charging stage) or decrease (during the discharging stage) relative to OCV.

As indicated by eqs 3 and 4, an increase in stack resistance decreases voltage efficiency. Therefore, given that ballast addition generally increased stack resistance, then ballast addition also correspondingly decreased voltage efficiency. Specifically, ballast addition reduced the voltage efficiency from 39.4% in the case of no ballast to 36.0% and 24.0% when mono-EG and tetra-EG, respectively, were added at their highest concentrations. The much greater reduction in voltage efficiency associated with tetra-EG compared to mono-EG is consistent with the larger decrease in solution conductivity associated with tetra-EG (see previous section).

Open Circuit Voltage and Round-Trip Energy Efficiency. The impact of ballast addition to the dilute salt solution on the initial OCV of the stack is depicted in Figure 2e. The results indicate that ballast addition to the dilute salt solution decreased the initial stack OCV, particularly in the case of tetra-EG. The OCV is defined as the battery voltage when no current is flowing, and for (reverse) electrodialysis systems can be calculated from the Nernst equation as[17]

$$\mathrm{OCV} = \alpha\frac{RT}{zF}\ln\frac{\gamma_C C_C}{\gamma_D C_D} \quad (5)$$

where α (dimensionless) is the membrane permselectivity, F is the Faraday constant (96,485 $C.mol^{-1}$), z (dimensionless) is the charge of the counterion (+1 for CEM and −1 for AEM in this case), C_C and C_D (M) are the concentrations of the counterion in the concentrated and dilute solutions, respectively, and γ_C and γ_D (dimensionless) are the activity coefficients of the counterion in the concentrated and dilute solutions, respectively. Given that in our tests, all experimental variables in eq 5 were held constant, except for the dilute solution activity coefficient γ_D, then eq 5 suggests that the decrease in OCV observed upon ballast addition could be explained by an increase in γ_D, and/or a decrease in membrane permselectivity. However, a significant increase in γ_D is not plausible because the activity coefficient of NaCl is known to decrease in mixed solvent systems containing water and either ethylene glycol or glycerol.[18] Moreover, the activity coefficients were previously observed[18] not to be significantly different from those in pure aqueous solution when the mass fraction of mono-EG was below 40% (compared to only 3−6% in this work). Thus, one must conclude that ballast addition resulted in a change in membrane permselectivity, α, as defined by eq 5. While this conclusion is consistent with previous studies showing that α is a function of water quality,[19−21] α is effectively a correction factor that accounts for any deviation between the measured OCV and that calculated with the Nernst equation. Therefore, concluding that ballast addition resulted in a change in membrane permselectivity does not explain from a fundamental perspective why ballast addition affected OCV.

Toward achieving a more fundamental understanding of why OCV decreased upon ballast addition, we investigated whether changes in various solution properties could explain the observed reductions in OCV. As shown in Figure 3, we

DOI: 10.1021/acs.est.6b03720
Environ. Sci. Technol. 2017, 51, 1910−1917

observed a strong linear correlation (R^2 = 0.961) between OCV and the volume fraction of ballast in the dilute salt solution.

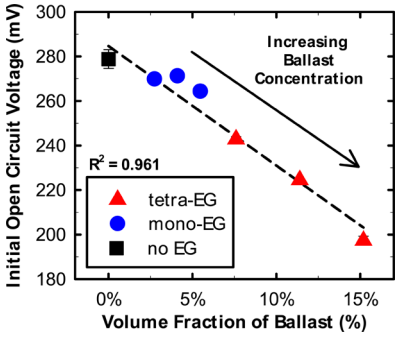

Figure 3. Relationship between the volume fraction of ballast in the dilute salt solution and the measured stack OCV. Data points and error bars (some of which are covered by the symbols) represent the average and standard deviation, respectively, of two replicates. The dashed line is a linear regression through the combined no EG, mono-EG, and tetra-EG data.

This finding led us to hypothesize that the ballasted salt solution was in fact a two-phase mixture in which the salt was present exclusively in the aqueous phase. This means that higher volume fractions of ballast would confine the salt to smaller volumes, effectively increasing its molar concentration in the dilute salt solution and lowering its concentration gradient across the membranes.

Previous studies of salt-water-glycol mixtures[18] expressed salt concentration on the molal scale (i.e., mol per kg of water in the mixture) rather than the molar scale, a choice which would reflect that salts are only present in the aqueous (not ballast) phase. Since the ballast takes the place of water in the solution, the molal concentration of salt in the ballasted dilute solution increases with ballast addition. Accordingly, we compared the measured stack OCV to the predicted stack OCV calculated by replacing C_C and C_D in eq 5 with molal concentrations expressed per kg of water in the solution. For the calculations, we used the α determined from the OCV with no ballast. As shown in Figure 4, the predicted OCV was within only 8% of the measured value for all conditions tested. This result

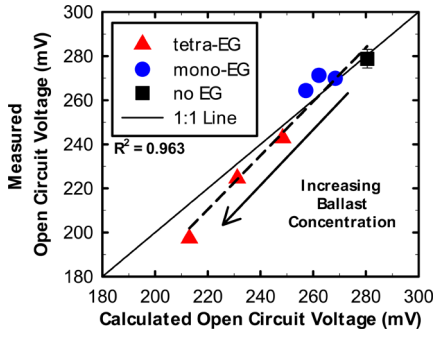

Figure 4. Comparison of measured and predicted initial stack OCV. The predicted OCV was calculated with eq 5 by replacing C_C and C_D with molal concentrations. The solid 1:1 line indicates perfect correspondence between the measured and predicted values, and the dashed line represents a linear correlation between the combined no EG, mono-EG, and tetra-EG data. Data points and error bars (some of which are covered by the symbols) represent the average and standard deviation, respectively, of 2 replicates.

provides strong evidence that our partitioning hypothesis is correct, and illustrates that the molal concentration scale must be used to predict changes in OCV associated with ballast addition.

Although the close agreement between the measured and predicted OCV (Figure 4) provides strong support for the partitioning hypothesis, we note that because OCV scales with volume fraction of ballast, it also scales with other properties of the ballasted solution. For example, OCV was strongly correlated with weight fraction of ballast (R^2 = 0.961), density (R^2 = 0.965), relative permittivity (R^2 = 0.990), and viscosity (R^2 = 0.996, see Supporting Information). Therefore, the changes in these solution properties represent potential alternative explanations to the OCV reductions. Regardless of which is the fundamental reason for these OCV reductions, the strong correlations observed between OCV and solution properties provide strong evidence that the observed OCV reductions are related to changes in bulk solution properties, not to changes in membrane permselectivity (α).

Finally, we consider the round-trip energy efficiency. As indicated by eq 4, the OCV impacts the total battery voltage E, which represents the energy per unit of charge that is either consumed by the battery during charging or extracted from the battery during discharging. Given that ballast addition lowered the OCV, eq 4 also indicates that ballast addition reduces E (though modestly), meaning that a greater proportion of E is associated with energy lost to resistance. Thus, the presence of ballast has a negative impact on voltage efficiency. On the other hand, as shown above (Figure 2b), the use of ballast had a significant positive impact on the faradaic energy efficiency.

The combined effect of these competing impacts (reduced voltage efficiency and improved faradaic efficiency) can best be assessed through the round-trip energy efficiency. The round-trip energy efficiency (η, dimensionless) is defined as the ratio between the amount of energy that is released during discharging and the amount of energy stored by the battery during charging. Round-trip energy efficiency can be calculated as[13]

$$\eta = \eta_I \eta_V = \frac{\int_0^{t_d} E_d I_d dt}{\int_0^{t_c} E_c I_c dt} \quad (6)$$

As shown in Figure 2f, the round-trip energy efficiency increased monotonically with ballast concentration, from 7% with no ballast to 11% and 18% for mono-EG and tetra-EG, respectively, at the maximum ballast concentrations used. However, as noted above, sustainable operation can only be achieved when water transport between the concentrated and dilute salt solutions is near zero, or at approximately 125% of $C_{B,OB}$ for tetra-EG. This concentration would correspond to a round-trip energy efficiency of approximately 15%, which is more than twice that achieved with no ballast. Therefore, in general, the dramatic improvements in faradaic efficiency that resulted from added ballast more than compensated for the reductions in voltage efficiency.

It should be noted that the low round-trip energy efficiencies reported in this work (7−15%) are a reflection of our selection of stack components and geometry, and are not optimized. In previous work,[2] a round-trip efficiency of 34% was achieved without ballast using similar conditions and more optimized components (e.g., low-resistance membranes and thin fluid compartments to achieve a lower stack resistance). Since the

DOI: 10.1021/acs.est.6b03720
Environ. Sci. Technol. 2017, 51, 1910−1917

osmotic ballasts primarily improve the faradaic efficiency while only modestly increasing the stack resistance, one would expect a similar doubling of round-trip efficiency to occur in a more optimized system, suggesting that a round-trip efficiency greater than 60% may be feasible in the near future. At this level, the concentration battery would approach the near-term performance target of 75% articulated by the U.S. Department of Energy for grid-scale energy storage systems.[22]

Ballast Crossover from Dilute to Concentrated Salt Solution. As noted above, the most effective control of osmosis was achieved using ballast concentrations in the dilute salt solution considerably higher than those required to achieve osmotic balance with the concentrated salt solution (125% of $C_{B,OB}$ for tetra-EG and >200% of $C_{B,OB}$ for mono-EG). A potential explanation for this observation is ballast crossover (i.e., diffusion) from the dilute to the concentrated salt solution through the ion exchange membranes. Ballast crossover would reduce the effective osmotic pressure of the ballasted solution and increase the osmotic pressure of the concentrated salt solution. To test this hypothesis, we measured for each test the net amount of ballast transported from the dilute to the concentrated salt compartments throughout the complete charge–discharge cycle (Figure 5).

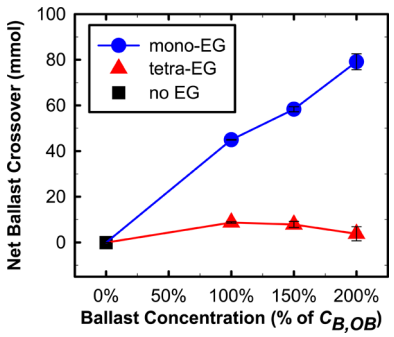

Figure 5. Net amount of ballast crossover from the dilute to the concentrated salt solution compartment as a function of initial ballast concentration in the dilute salt solution. Data points and error bars (some of which are covered by the symbols) represent the average and standard deviation, respectively, of two replicates.

The results in Figure 5 show that the maximum amounts of crossover of mono-EG and tetra-EG were 79.1 and 8.7 mmol, respectively. These amounts represent approximately 45% (mono-EG) and 11% (tetra-EG) of the total amount of ballast initially present in the dilute salt solution. The observed difference in crossover of mono-EG compared to that of tetra-EG is consistent with the higher molecular weight and lower diffusivity of tetra-EG compared to those of mono-EG (see Table 1), since higher molecular weight and lower diffusivity would result in higher rejection by the ion exchange membranes.

Figure 5 also shows that the crossover of mono-EG increased linearly with the amount of ballast added. This indicates that for mono-EG, the ballast concentration was the main factor determining ballast crossover. By contrast, in the case of tetra-EG, ballast crossover did not have a linear relationship to initial ballast concentration in the dilute salt solution, but rather maximum crossover occurred at 100% of $C_{B,OB}$ and approached 0 at 200% of $C_{B,OB}$. Therefore, in addition to the initial ballast concentration in the dilute salt solution, additional factors affected ballast crossover for the tetra-EG case. One potential such factor is the direction of osmosis during experiments. As observed in Figure 2a, while for all concentrations of mono-EG, osmosis occurred in the same direction as net ballast crossover (i.e., from the dilute to the concentrated salt solution), for tetra-EG, osmosis occurred in the opposite direction to net ballast crossover at 150% and 200% of $C_{B,OB}$. Therefore, we conclude that for tetra-EG inverted osmosis slowed down the net rate of ballast crossover through the membrane.

Overall, our results show that a noncharged ballast that is effectively retained by the ion exchange membranes in a closed-loop RED-based energy storage system can significantly enhance its performance. Specifically, ballast addition to the dilute solution resulted in a substantial increase in faradaic energy efficiency, which was primarily a result of decreased osmosis. Similar benefits may be derived by applying this approach in other closed-loop, aqueous energy processes such as RED systems proposed for waste heat recovery[23,24] and aqueous-based redox flow batteries. Further study of this concept may lead to the identification or development of optimized ballasts that are more effectively rejected by ion exchange membranes and have a lower impact on solution conductivity.

■ ASSOCIATED CONTENT

Supporting Information

The Supporting Information is available free of charge on the ACS Publications website at DOI: 10.1021/acs.est.6b03720.

Estimation of theoretical amount of ballast required, determination of optimal current density, measurement of single membrane potential and single membrane resistance, comparison of measured stack resistance with predictions from individual membrane resistance and solution conductivity, correlations of initial open circuit voltage with various solution properties, calculation of water and ballast transport in charge–discharge cycles (PDF)

■ AUTHOR INFORMATION

Corresponding Author

*Phone: 1-919-966-9010; fax: +1-919-966-7911; e-mail: coronell@unc.edu].

ORCID

Ryan S. Kingsbury: 0000-0002-7168-3967

Orlando Coronell: 0000-0002-7018-391X

Notes

The authors declare no competing financial interest.

■ ACKNOWLEDGMENTS

This work was funded by the University of North Carolina Research Opportunities Initiative (ROI) program. We also wish to acknowledge Dr. Douglas Call and Dr. Fei Liu (North Carolina State University) and Dr. Shan Zhu (University of North Carolina) for helpful discussions.

■ REFERENCES

(1) Alotto, P.; Guarnieri, M.; Moro, F. Redox flow batteries for the storage of renewable energy: A review. *Renewable Sustainable Energy Rev.* **2014**, *29*, 325–335.

(2) Kingsbury, R. S.; Chu, K.; Coronell, O. Energy storage by reversible electrodialysis: The concentration battery. *J. Membr. Sci.* **2015**, *495*, 502–516.

DOI: 10.1021/acs.est.6b03720
Environ. Sci. Technol. 2017, 51, 1910–1917

(3) van Egmond, W. J.; Saakes, M.; Porada, S.; Meuwissen, T.; Buisman, C. J. N.; Hamelers, H. V. M. The concentration gradient flow battery as electricity storage system: Technology potential and energy dissipation. *J. Power Sources* **2016**, *325*, 129−139.
(4) Veerman, J.; de Jong, R. M.; Saakes, M.; Metz, S. J.; Harmsen, G. J. Reverse electrodialysis: Comparison of six commercial membrane pairs on the thermodynamic efficiency and power density. *J. Membr. Sci.* **2009**, *343* (1−2), 7−15.
(5) Veerman, J.; Saakes, M.; Metz, S. J.; Harmsen, G. J. Electrical power from sea and river water by reverse electrodialysis: a first step from the laboratory to a real power plant. *Environ. Sci. Technol.* **2010**, *44* (23), 9207−9212.
(6) Yip, N. Y.; Vermaas, D. A.; Nijmeijer, K.; Elimelech, M. Thermodynamic, energy efficiency, and power density analysis of reverse electrodialysis power generation with natural salinity gradients. *Environ. Sci. Technol.* **2014**, *48*, 4925−4936.
(7) Bar, D., Ameridia Corporation. Personal Communication. 2016.
(8) Altmeier, P., PCCell GmbH. Personal Communication. 2016.
(9) Yue, H.; Zhao, Y.; Ma, X.; Gong, J. Ethylene glycol: properties, synthesis, and applications. *Chem. Soc. Rev.* **2012**, *41* (11), 4218.
(10) MEGlobal. Ethylene Glycol Product Guide. Form No: 001−00005−0508-CRCG. 2008; http://www.meglobal.biz/media/product_guides/MEGlobal_MEG.pdf (accessed July 24, 2016).
(11) Dow Chemical. Tetraethylene Glycol Product Guide. Form No: 612−00005−0207X CRCG. 2007; http://msdssearch.dow.com/PublishedLiteratureDOWCOM/dh_0952/0901b8038095238b.pdf?filepath=ethyleneglycol/pdfs/noreg/612-00005.pdf&fromPage=GetDoc (accessed July 24, 2016).
(12) Strathmann, H. *Introduction to Membrane Science and Technology*; Wiley-VCH Verlag: Weinheim, Germany, 2011.
(13) Lu, R.; Yang, A.; Xue, Y.; Xu, L.; Zhu, C. Analysis of the key factors affecting the energy efficiency of batteries in electric vehicle. *World Electr. Veh. J.* **2010**, *4* (2), 9−13.
(14) Robinson, R. A.; Stokes, R. H. *Electrolyte Solutions*: Second *Revised ed.*; Butterworths: London, 1968.
(15) Sata, T.; Mine, K.; Matsusaki, K. Change in Transport Properties of Anion-Exchange Membranes in the Presence of Ethylene Glycols in Electrodialysis. *J. Colloid Interface Sci.* **1998**, *202* (2), 348−358.
(16) Sata, T.; Tanimoto, M.; Kawamura, K.; Matsusaki, K. Transport Properties of Cation Exchange Membranes in the Presence of Ether Compounds in Electrodialysis. *J. Colloid Interface Sci.* **1999**, *219* (2), 310−319.
(17) Helfferich, F. *Ion Exchange*; McGraw-Hill: New York, 1962.
(18) Kraus, K. A.; Raridon, R. J.; Baldwin, W. H. Properties of Organic-Water Mixtures. I. Activity Coefficients of Sodium Chloride, Potassium Chloride, and Barium Nitrate in Saturated Water Mixtures of Glycol, Glycerol, and Their Acetates. Model Solutions for Hyperfiltration Membranes. *J. Am. Chem. Soc.* **1964**, *86*, 2571.
(19) Daniilidis, A.; Vermaas, D. A.; Herber, R.; Nijmeijer, K. Experimentally obtainable energy from mixing river water, seawater or brines with reverse electrodialysis. *Renewable Energy* **2014**, *64*, 123−131.
(20) Geise, G. M.; Cassady, H. J.; Paul, D. R.; Logan, E.; Hickner, M. A. Specific ion effects on membrane potential and the permselectivity of ion exchange membranes. *Phys. Chem. Chem. Phys.* **2014**, *16*, 21673−21681.
(21) Cassady, H. J.; Cimino, E. C.; Kumar, M.; Hickner, M. A. Specific ion effects on the permselectivity of sulfonated poly(ether sulfone) cation exchange membranes. *J. Membr. Sci.* **2016**, *508*, 146−152.
(22) U.S. Department of Energy. *Grid Energy Storage*. 2013; http://energy.gov/oe/downloads/grid-energy-storage-december-2013 (accessed October 6, 2016).
(23) Kwon, K.; Park, B. H.; Kim, D. H.; Kim, D. Parametric study of reverse electrodialysis using ammonium bicarbonate solution for low-grade waste heat recovery. *Energy Convers. Manage.* **2015**, *103*, 104−110.
(24) Luo, X.; Cao, X.; Mo, Y.; Xiao, K.; Zhang, X.; Liang, P.; Huang, X. Power generation by coupling reverse electrodialysis and ammonium bicarbonate: Implication for recovery of waste heat. *Electrochem. Commun.* **2012**, *19*, 25−28.

DOI: 10.1021/acs.est.6b03720
Environ. Sci. Technol. 2017, 51, 1910−1917